MECHANICAL PROPERTIES, CORROSION RESISTANCE AND MICROSTRUCTURE OF BOTH REGULAR AND TITANIUM HARDENED 625 ALLOYS

R. Cozar, M. Rouby, B. Mayonobe, C. Morizot

TECPHY, 58160 Imphy, France

ABSTRACT

The addition of titanium to standard 625 grade enhances the age-hardening response, enabling yield strengths greater than 800 MPa to be obtained by simple, industrially compatible, heat treatments. The effect of such treatments on microstructure have been studied, together with their influence on the strength/toughness trade-off and the resistance to intergranular corrosion, compared to regular 625 alloy.

Superalloys 718, 625 and Various Derivatives
Edited by Edward A. Loria
The Minerals, Metals & Materials Society, 1991

1. Introduction

Alloy 625 combines excellent corrosion resistance in a large number of aggressive environments with attractive mechanical properties. Solid solution hardening, chiefly by high molybdenum and niobium contents, ensures a proof stress greater than 414 MPa (minimum grade 1 specification) for an annealed fine grained structure. However, certain applications require a proof stress of 800 MPa or more, and in the standard grade this level can only be attained in thin cold-worked products. For more massive parts, it has been endeavoured to obtain these characteristics by precipitation hardening, the alloy composition being modified in order to limit the aging treatments to industrially acceptable times. The elements capable of combining with nickel to produce homogeneous precipitation of γ'' or γ' phases are principally Nb, Ti and Al. It was preferred not to increase the amount of niobium, due to its strong tendency to segregate during solidification. A preliminary study having shown that aluminium is less efficient than titanium, it was decided to raise the concentration of this element by about 1 weight % ($\simeq$ 0.2 % Ti in the standard grade). A similar alloy has been developed by R.B. Frank and T.A. De Bold [1,2].

In order to improved knowledge of this material, a study was undertaken on the solidification structure, together with the influence of annealing and aging treatments on the microstructure, mechanical properties and corrosion resistance. Since the alloy is liable to be used at high temperatures, prolonged aging was carried out between 550 and 750°C for periods up to about 2000 hours.

2. Materials and experimental techniques

2.1. Materials

The investigations were performed on three 50 kg vacuum induction melted laboratory heats, two corresponding to the hardened grade (A and B in table I), and the third having a composition in the standard range for alloy 625 (heat C). Slices were cut from the bottom of ingots B and C for a comparative study of the solidification structures. The remainder of the metal was processed by forging and hot rolling to 15 mm diameter bar, from which the various test specimens were cut.

Alloy	C	Ni	Cr	Fe	Nb	Mo	Ti	Al	Si
A	0.035	60.71	19.65	4.79	3.95	8.16	1.13	0.10	0.09
B	0.026	60.18	19.89	4.66	3.70	8.26	1.21	0.15	0.07
C	0.034	61.97	20.02	4.70	3.77	8.21	0.33	0.27	0.05

Table I : Composition of the experimental alloys (wt. %)

2.2. Solidification structure and homogenization

Specimens taken from a mid-radius position in the slices of ingots B and C were mechanically polished to 1 µm diamond paste and examined by optical microscopy, before being studied in a scanning electron microscope (ZEISS DSM 950) equipped with EDS (LINK AN 10 000) and WDS (MICROSPEC WDX-2A) spectrometers. Back-scattered electron imaging, with high atomic number contrast (V = 10 kV, I ~ 7 nA), clearly reveals the dendrite network (figure 1). The heavy elements (Nb and Mo) segregated to the interdendritic spaces show up bright, whereas the dendrites appear dark. However, differences in grey-level are readily discernible in both types of zone, facilitating the choice of areas for determining the maximum degree of segregation. After having identified such regions, the microscope parameters were adjusted for EDS point analysis (in particular, V = 20 kV, I ~ 1 nA).

The effect of a homogenization treatment at 1180°C and the uniformity of the composition of the hot-rolled bars were also studied.

2.3. Mechanical properties

The hardening kinetics were first determined for alloy A by measuring HV30 values on specimens treated for 1 to 81 hours between 600 and 800°C, after prior annealing for 1 hour at 950°C, followed by a water quench. The hardening effects of step-aging treatments ("θ, t" + 50°C/h cool to 620°C + 8 h hold), with 700°C $\leq \theta \leq$ 760°C and 8 h $\leq$ t $\leq$ 24 h, were studied by hardness and room temperature tensile testing.

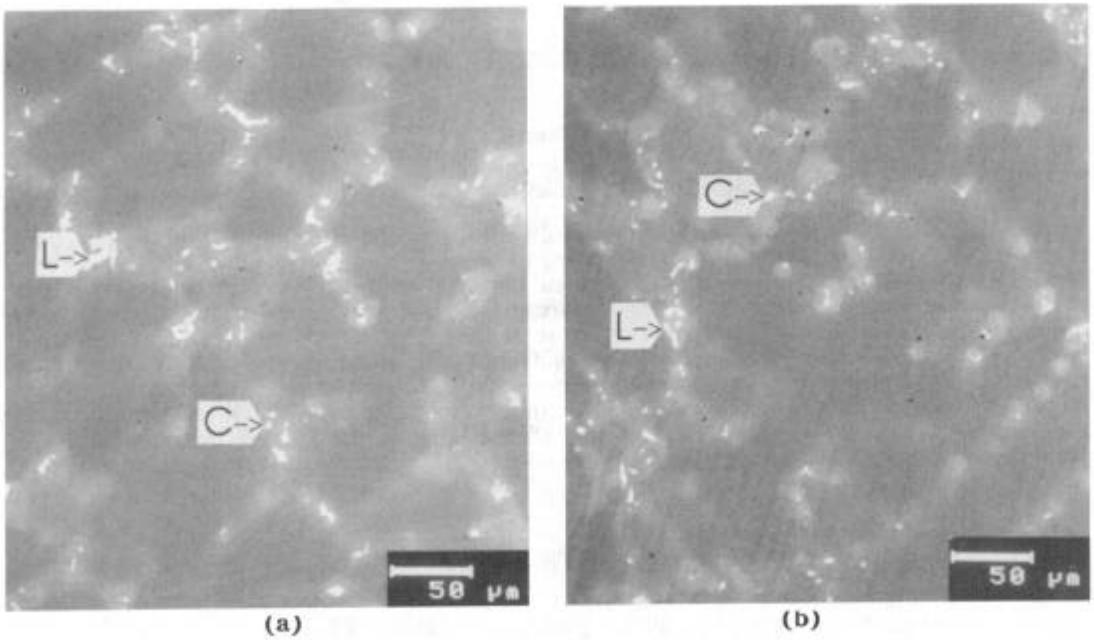

(a) (b)

Figure 1 : Back-scattered electron images of polished sections, showing the dendrite structure in alloys B (a) and C (b).

For alloys B and C, specimens taken from the rolled bars were annealed for 1 hour between 900 and 1150°C, then water quenched, in order to study the influence of such treatments on the microstructure (grain size and phase constitution) and mechanical properties (impact strength and tensile behaviour) in the unaged condition. For alloy B, the specimens annealed as indicated above were hardened by the step-aging sequence 750°C 8 h + 50°C/h cool to 620°C + 8 h hold + air cool (750°C 8 h -> 620°C 8 h), and the tensile and impact characteristics were determined, in order to define the solution treatment corresponding to an optimum compromise between proof stress and toughness.

2.4. Prolonged aging

The hardening kinetics between 550 and 750°C were determined for alloy B on specimens aged for periods from 2 to 2048 hours, after prior annealing for 1 hour at 1050°C, followed by a water quench. The long holding times enabled the overaging behaviour of the hardened grade to be studied at the highest temperatures. Alloy C was also subjected to long-time aging at lower temperatures (550 and 580°C), in order to compare the behaviour of the two materials in the temperature range where standard 625 alloy, used in the initially annealed or slightly cold-worked condition, can undergo precipitation hardening in service.

2.5. Corrosion resistance

The investigations were concentrated essentially on the intergranular corrosion resistance of alloy B in different annealed and annealed and aged conditions. The specimens were tested using the standard ASTM G 28 A procedure (boiling aqueous solution of 50 % sufuric acid and ferric sulfate). The weight losses measured after 24 or 120 hours exposure are converted to corrosion rates in mm/yr.

A few pitting corrosion tests were also carried out using the ASTM G 48 A method, which involves the determination of the critical pitting temperature, by 24 hour immersion in a 6 % aqueous ferric chloride solution. This medium must be acidified by adding HCl (pH = 0.5) to conserve its stability at temperatures above 50°C (up to around 100°C).

2.6. Microstructural examination and phase analysis

Several specimens were examined by optical and by scanning and transmission electron microscopy. In particular, the phases present were revealed either on polished and etched sections, on thin foils, or on carbon extraction replicas, enabling them to be

analyzed with the EDS spectrometer (LINK AN 10 000) associated with the transmission microscope (JEOL 2000 FX).

3. Results

3.1. Solidification structure and homogenization

Figure 1 shows that the dendrite structure in alloys B and C is similar, and while the interdendritic spaces contain almost identical amounts of MC carbide (C), a much higher density of Laves phase (L) is present in those of alloy B. Point analyses in the dendrites and spaces show that the composition of both types of region can vary greatly. The maximum segregation was determined in areas showing the greatest contrast in back-scattered electron images (table II). Calculations of the segregation coefficient I_s (interdendritic concentration/dendrite concentration) and the partition coefficient k (dendrite concentration/nominal concentration) clearly show that the elements Mo, Ti, and especially Nb, are preferentially rejected into the interdendritic liquid during solidification. In the dendrite centers, the niobium content varies between about 1.4 and 2.7 %, compared to 5 to 8 % in the spaces.

Alloy	Zones analyzed	Ni	Cr	Fe	Nb	Mo	Ti
B	nominal composition(1)	60.2	19.9	4.66	3.70	8.26	1.21
	dendrites (2)	63.7	20.7	5.09	1.42	7.03	0.82
	spaces (3)	56.9	18.3	3.92	7.31	9.54	1.70
	Is = (3)/(2)	0.89	0.88	0.77	5.2	1.36	2.07
	K = (2)/(1)	1.06	1.04	1.09	0.38	0.85	0.68
C	nominal composition(1)	62.0	20.0	4.70	3.77	8.21	0.33
	dendrites (2)	64.3	20.6	4.96	1.39	7.01	0.26
	spaces (3)	57.6	18.2	4.08	7.54	10.16	0.41
	Is = (3)/(2)	0.90	0.88	0.86	5.4	1.45	1.58
	K = (2)/(1)	1.04	1.03	1.06	0.37	0.85	0.79

Table II : Extreme compositions (wt. %) in the dendrites (mean of the two zones with the lowest Nb contents) and in the interdendritic spaces (mean of the two zones with the highest Nb contents) for alloys B and C, together with the nominal compositions.

Table III summarizes the results of point analyses performed on the Laves phase and MC carbides (analysis of M) in alloys B and C. It is noteworthy that, in both cases, the titanium content is proportional to that in the alloy. The dark particles visible in the micrographs of figure 1 are niobium-containing titanium nitrides.

Homogenization treatment at 1180°C enables the Laves phase to be eliminated in these two alloys, and after holding for 15 hours, the segregation coefficient for niobium, I_s(Nb), is of the order of 1.10 for alloy C and 1.13 for alloy B. The MC carbides and the Ti-Nb nitrides are still present. These particles are also observed in the hot-rolled bars, in which a fine dispersion of secondary MC carbides, formed during processing, is also found. In these products, the distribution of niobium in the matrix is homogeneous.

3.2. Precipitation hardening

Figure 2 shows that a stepped aging treatment applied to alloy A produces a marked increase in hardness (Δ $HV30_{max}$ ~ 190) for a total treatment time of about 18 hours. Maximum hardening is obtained for the treatment 750°C 8 h -> 620°C 8 h. This same treatment also leads to the highest proof stress (0.2 % P.S. = 1070 MPa, cf. table IV).

Phase	Alloy	Ni	Cr	Fe	Nb	Mo	Ti	Si
Laves	B	42.9	22.1	4.0	15.1	13.8	1.3	0.7
	C	44.6	20.6	3.4	14.9	14.2	0.4	1.2
MC	B	-	1.0	-	78.3	6.2	14.5	-
	C	-	0.7	-	87.5	4.4	7.1	-

Table III : **Analysis (at. %) of the phases present in the as-solidified condition.**

Heat treatment	0.2 % P.S. (MPa)	KCV at 20°C (daJ/cm²)
950°C 1h WQ (1)	448	21.5
(1) + 720°C 8h, 50°C/h cool -> 620°C 8h	976	8.7
(1) + 720°C 24h " " "	1036	7.5
(1) + 750°C 8h " " "	1070	6.9
(1) + 750°C 24h " " "	1038	6.8

Table IV : **Alloy A : variation of proof stress and impact strength at 20°C with heat treatment.**

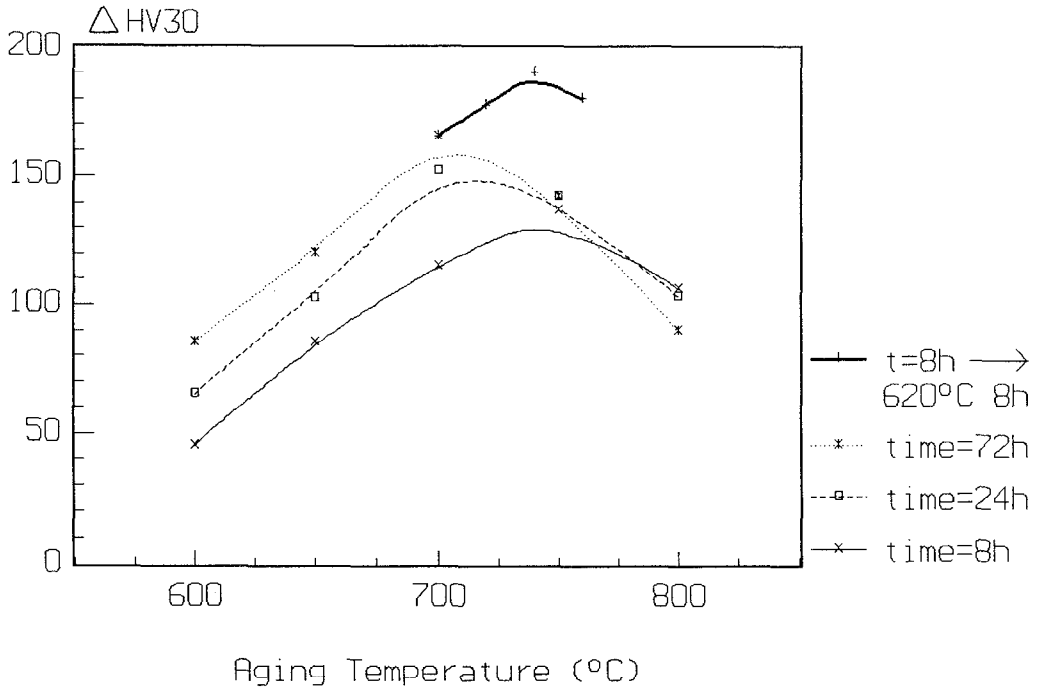

Figure 2 : **Alloy A : increase in hardness during isothermal treatments of 8, 24 and 72 hours and by step aging 8h, 50°C/h cool to 620°C 8h.**

Figure 3 shows that the proof stress falls rapidly for alloys B and C when the annealing temperature increases from 900 to 1000°C. At higher temperatures, the variation is smaller and can be related to grain growth through the expression : 0.2 % P.S. = 15.8 $D^{-1/2}$ + 300 (0.2 % P.S. in MPa and D, the mean grain diameter, in mm). For annealing treatments at or below 1000°C, the hot-rolling substructure is not completely eliminated and, for alloy B, the δ-Ni_3Nb phase precipitates both at the grain boundaries and in the matrix, particularly at 950°C. This phase is not present for annealing temperatures of 1050°C and above. In the precipitation hardened condition (750°C 8 h -> 620°C 8 h), the proof stress of alloy B increases by about 600 MPa, whatever the annealing temperature, and is always greater than 800 MPa (960 MPa ≤ 0.2 % P.S. ≤ 1270 MPa).

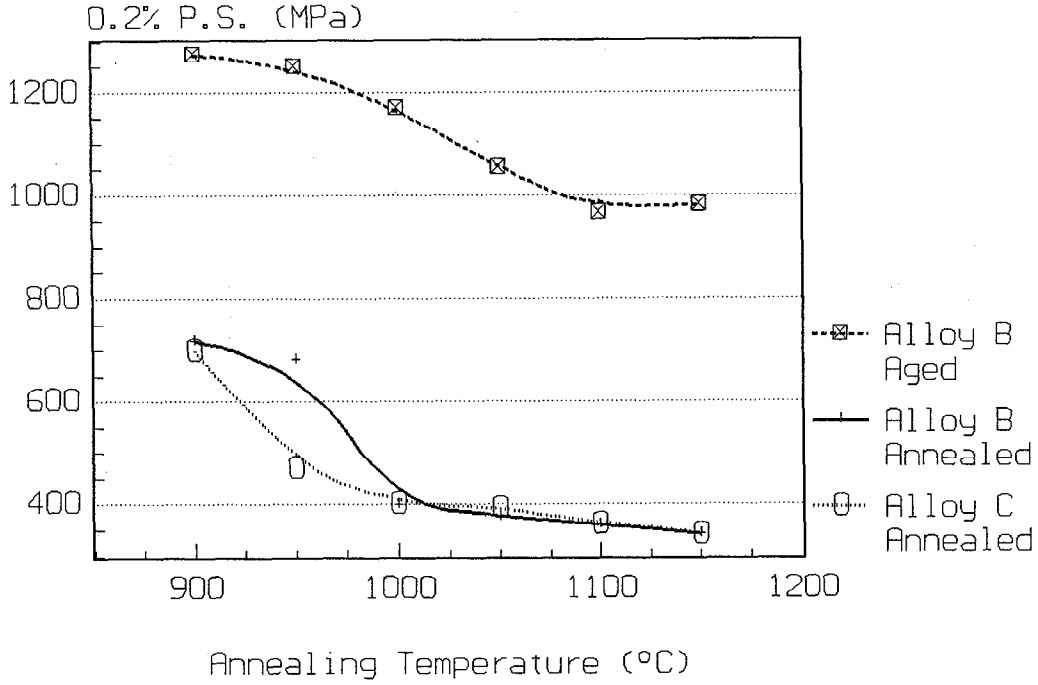

Figure 3 : Influence of annealing temperature on the proof stress in the annealed condition (alloys Band C) and after precipitation hardening (alloy B) obtained by step aging : 750°C 8h -> 620°C 8h

In figure 4, in which the 0.2 % P.S. is plotted as a function of the room temperature Charpy impact strength (KCV), the less ductile behaviour of alloy B in the annealed condition can be partly explained by the presence of δ phase for the lowest annealing temperatures, but a difference remains for the highest temperatures. In the hardened condition, the compromise between 0.2 % P.S. and KCV in alloy B is an optimum for annealing at 1050°C. At lower temperatures, the presence of δ phase exerts a deleterious influence, while, at higher temperatures (1100 and 1150°C), rupture becomes intergranular (figure 5). In effect, at these high temperatures, the secondary MC carbides are taken into solution and the grain size coarsens, leading to abundant precipitation, during aging, of M_6C and especially $M_{23}C_6$ carbides, which embrittle the grain boundaries.

3.3. Aging kinetics

Figure 6 shows that alloy B hardens at all temperatures between 550 and 750°C, at a rate which increases with temperature. Overaging occurs after only 15 hours at 750°C and after 200 hours at 700°C, but the hardness drops only slightly when treatment is continued. All of the thin foil observations for either short or long aging times between 650 and 750°C show that hardening is due solely to precipitation of the DO22-type body-centred tetragonal γ" phase, which is the principal source of strengthening in alloy 718 [3-5] and other alloys [6-8]. AEM/EDS analyses of this phase (table V) show that titanium and molybdenum substitute for niobium in the B sites of the A_3B compound. When the aging temperature decreases, the phase appears to become less stoichiometric, and chromium substitutes more extensively for nickel.

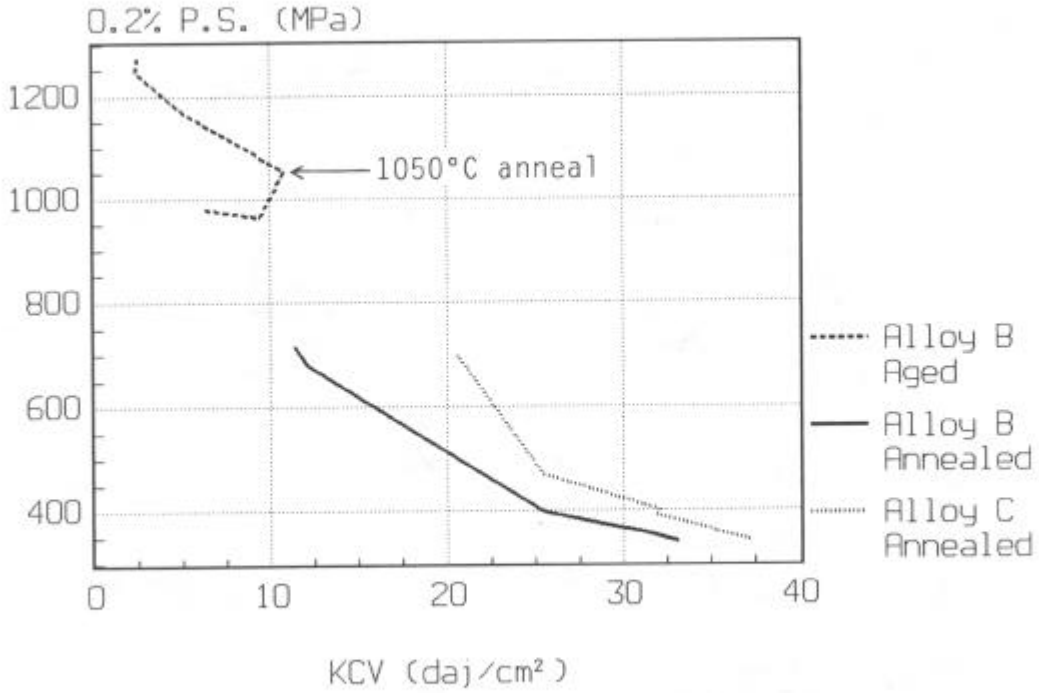

Figure 4 : **Relationship between proof stress and impact strength in the annealed (alloys B and C) and aged (alloys B : treatment 750°C 8h -> 620°C 8h) conditions.**

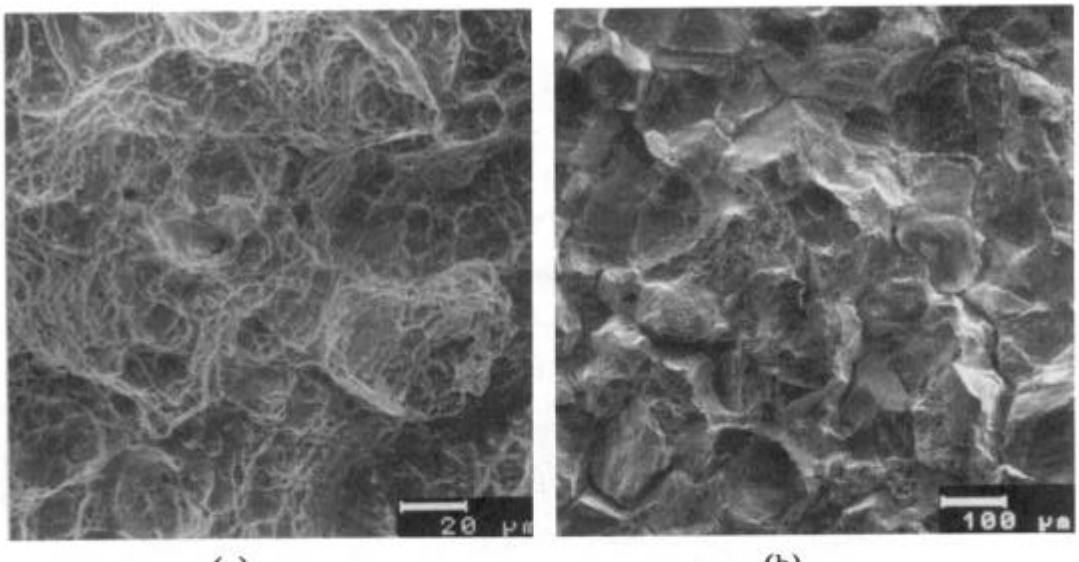

(a) **(b)**

Figure 5 : **Alloy B : Rupture surface of impact specimens annealed at (a) 1050°C and (b) 1150°C, then step-aged 750° C 8 h --> 620° C 8 h.**

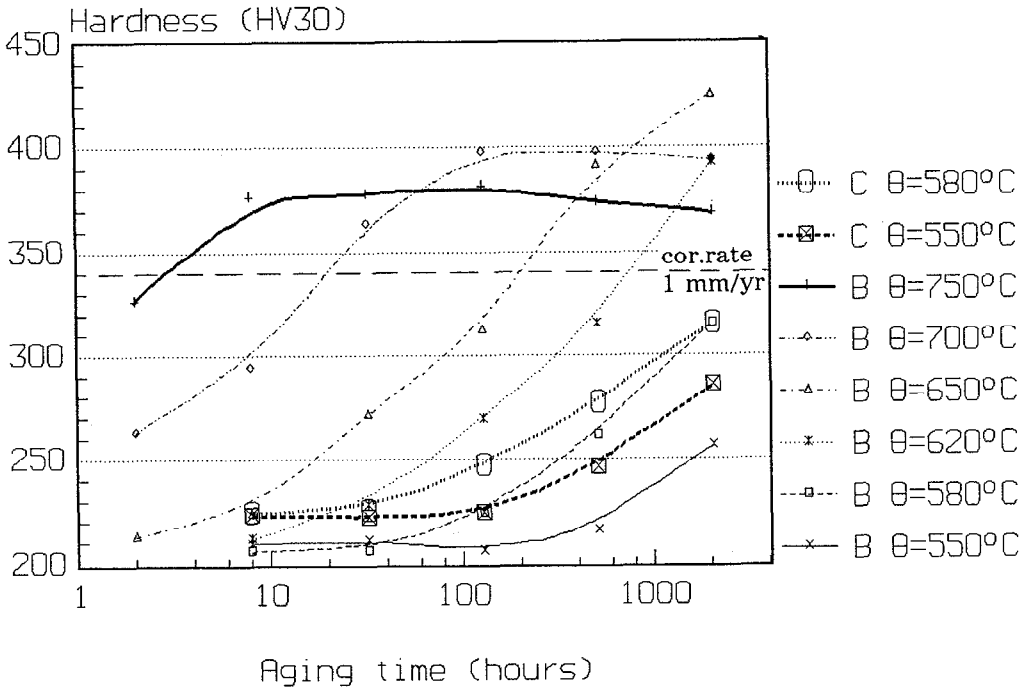

Figure 6 : **Alloy B : hardening kinetics between 550 and 750°C (initial condition : 1050°C 1h WQ)**
Alloy C : hardening kinetics at 550 and 580°C (initial condition : 1000°C 1h WQ)

		A			B				
Treatment	**Phase**	**Ni**	**Cr**	**Fe**	**Nb**	**Mo**	**Ti**	**Al**	**B**
(1) + 650°C 2048h	γ"	63.1	7.9	0.4	14.7	7.0	6.4	0.4	28.5
(1) + 750°C 2048h	γ"	71.0	4.4	0.7	12.7	4.4	6.3	0.4	23.8
(1) + 750°C 2048h	δ	71.9	3.9	0.5	12.7	6.2	4.8	-	23.7
950°C 1h WQ	δ	70	3	1	16	4	6	-	26

Table V : **Alloy B : AEM/EDS analyses of A3B-type γ" and δ phases (mean of at least 3 measurements). (1) : 1050°C 1h WQ.**

For exposures longer than 128 hours at 750°C, the metastable γ" phase partially decomposes, giving way to the stable δ phase (DOa-type orthorhombic structure), which precipitates throughout the grains in the form of long thin platelets (figure 7). It is noteworthy that the composition of this δ phase is very similar to that of the γ" , and also to that of the δ phase present in the specimens annealed at 950°C (table V). At 700°C, a few δ platelets are visible after 2048 hours, while for the same time at 650°C, only a fine dispersion of γ" phase is observed.

At low aging temperatures (550 and 580°C), hardening also occurs in alloy C, with kinetics similar to alloy B. The possibility of precipitation hardening in standard 625 alloy in the temperature range 600 to 800°C has already been reported [12-14], but with a smaller amplitude and at a slower rate than in alloy B, particularly for temperatures of 700°C and above.

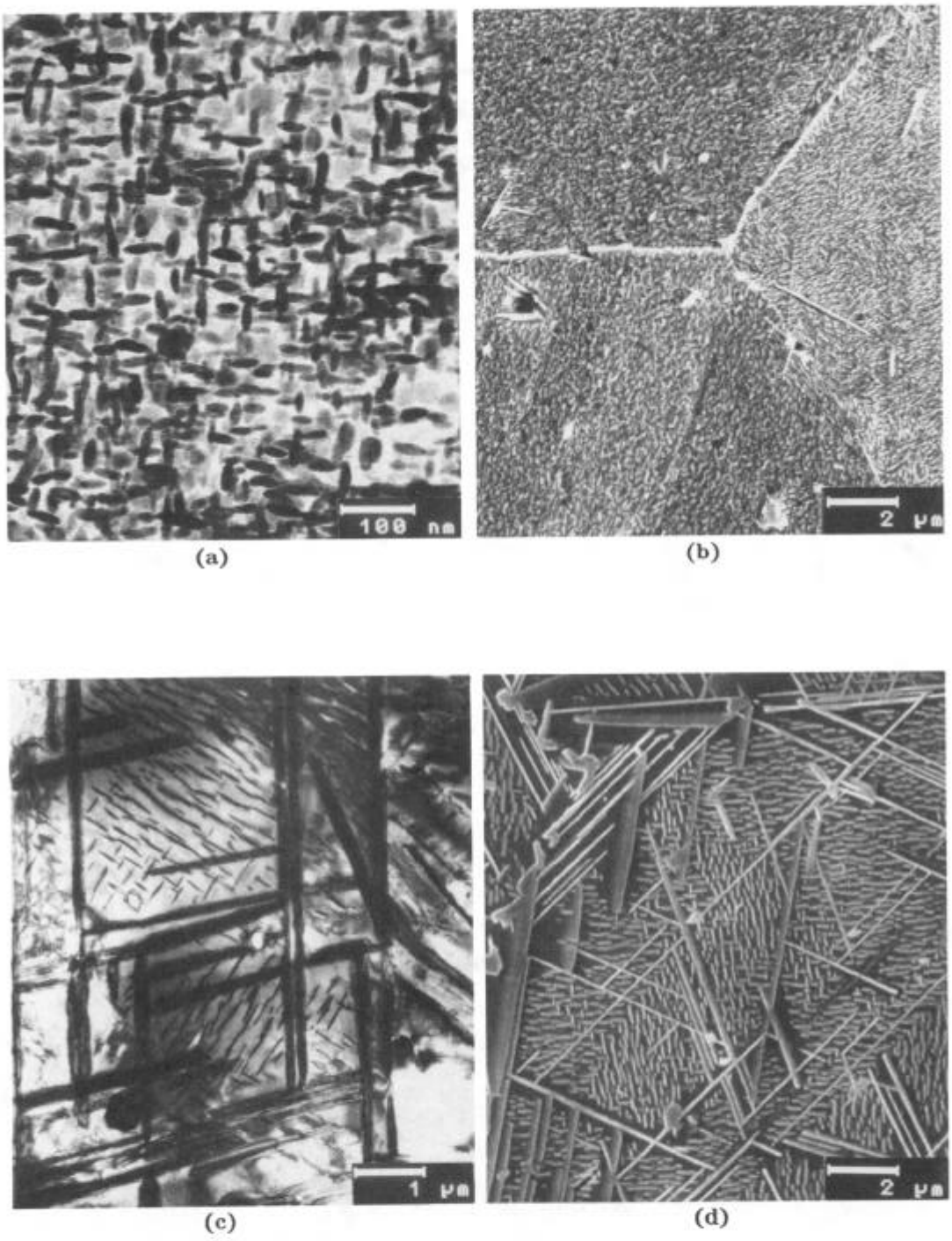

(a) (b)

(c) (d)

Figure 7 : Alloy B : Microstructure after aging for 2048 hours
(a) at 650°C (TEM image : γ" extracted on a carbon replica)
(b) at 700°C (SEM image : γ" and a few δ platelets)
(c,d) at 750°C [(c) TEM image on thin foil, (d) SEM image : γ" and long δ plates].

3.4. Corrosion resistance

Figure 8 shows that, in the annealed condition, the corrosion rate measured in the ASTM G 28 A test is slightly higher for alloy B treated at 950 and 1000°C. This suggests that the presence of δ phase has a deleterious influence on the behaviour in this test. In the age-hardened condition, the corrosion rate is significantly higher, going through a minimum for an annealing temperature of 1050°C, which also gave optimum mechanical properties (§ 3.2.). The tests carried out on the specimens used for the study of the aging kinetics (§ 3.3.) show that the corrosion rate increases with both the time and temperature of aging, and only the exposures at 550 and 580°C do not sensitize this grade (figure 9). For the higher temperatures, the times corresponding to a corrosion rate of 1 mm/yr give the same hardness in figure 6 (HV30 ~ 340). It is to be noted that this level was not attained after aging for 2048 hours at 550 and 580°C.

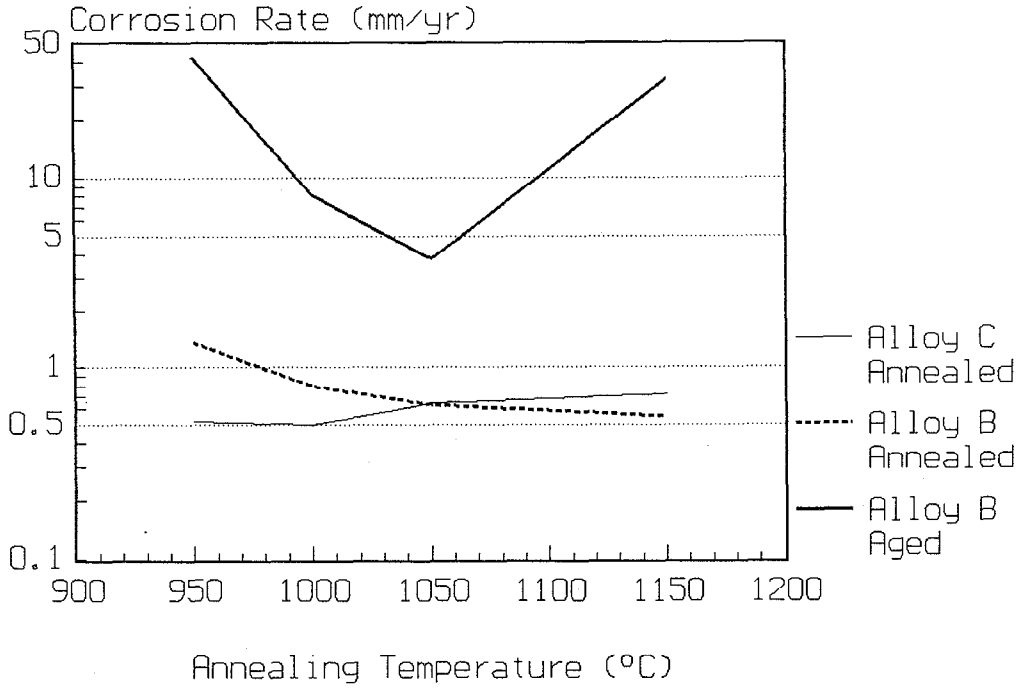

Figure 8 : Alloys B (annealed and aged* conditions) and C (annealed condition) : influence of annealing temperature on the corrosion rate in the ASTM G28A test.
*** 750°C 8h -> 620°C 8h**

The resistance to pitting corrosion seems to be less affected by aging than the intergranular corrosion behaviour, since the critical pitting temperature measured using the ASTM G 48 A test on alloy B, after the step aging treatment (750°C 8 h -> 620°C 8 h), is greater than 95°C, the same as for both alloys B and C in the annealed condition.

4. Discussion

4.1 Solidification and homogenization

The results presented in table II show that marked segregation occurs during solidification, particularly as regards niobium, for which the partition coefficient (k ~ 0.38) was found to be lower than that reported by Cieslak et al. (k ~ 0.50) for standard 625 alloy [9] and for Custom Age 625 Plus [10]. The nature of the phases present in the interdendritic spaces is in agreement with the known influence [9-11] of the elements C, Si and Nb. The low silicon level and relatively high carbon content in this grade explain the formation of MC carbide at the end of solidification (probably at about 1250°C), rather than M_6C carbides (which appear at about 1205°C for Si ~ 0.35 % and C ~ 0.01 %). In spite of the fairly high niobium concentration (~ 3.8 %),

the precipitation of MCcarbides limits the amount of Laves phase which forms subsequently, probably at around 1150°C, in alloy C. In alloy B, the addition of titanium does not modify the partition coefficient for niobium, but leads to a greater quantity of Laves phase, as was also observed in Custom Age 625 Plus [10]. In order to eliminate this phase, which can have a harmful effect on the alloy's hot-workability, it is important to take it into solution and to homogenize the microstructure by annealing at a temperature above 1150°C. It should be noted that the quantity of carbides and Laves phase formed during solidification can be decreased by reducing the silicon content and by limiting the C, Nb and Mo levels [1,2,9,10].

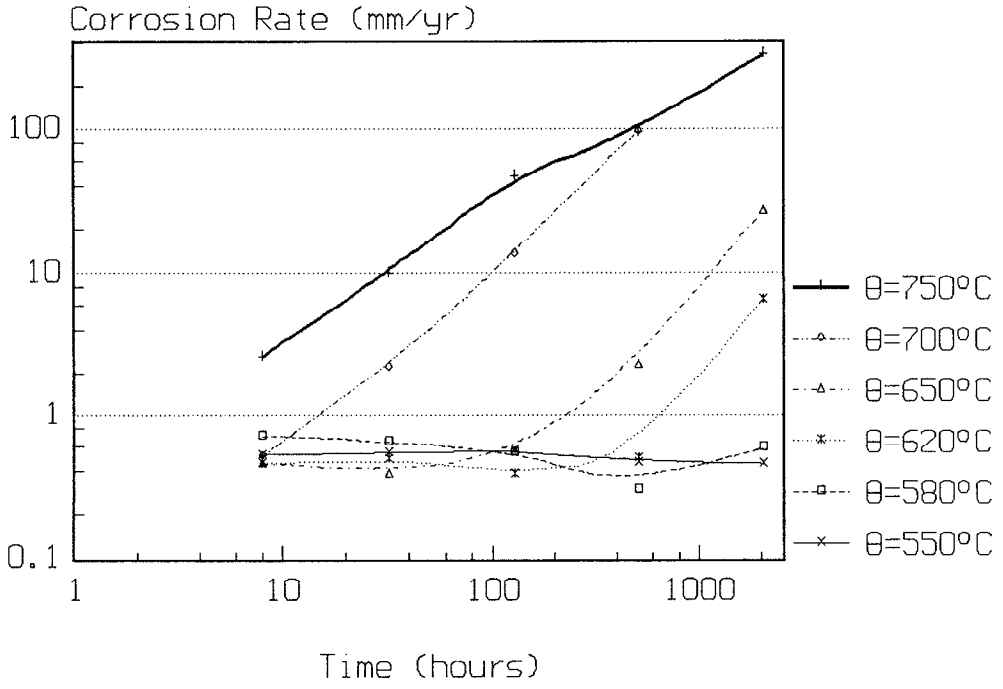

Figure 9 : Alloy B : influence of the time and temperature of aging on the corrosion rate in the ASTM G28A test (initial condition : 1050°C 1h WQ).

4.2 Precipitation hardening

The addition of titanium to 625 alloy produces a marked increase in the amplitude and rate of hardening, particularly in the temperature range 700 to 750°C, enabling proof stresses greater than 800 MPa to be obtained by step aging treatments of limited duration. This hardening is due to the homogeneous precipitation of the DO22-type body-centred tetragonal γ" phase. Contrary to 718 alloy, which contains the same hardening elements (Nb, Mo, Ti and Al) in different proportions, and where the γ' and γ" phases coexist [3-5,8], the γ' phase was not detected. The titanium, which is known to promote the formation of the $Ni_3(Ti,Al)$ γ' phase in Ni or Fe-Ni base alloys [15-17], contributes to hardening in this alloy by substituting for niobium in the B sites of the A_3B compound. A high concentration of titanium is not essential for the formation of γ", since it can also occur in the standard grade [12-14].

Long exposures at 700°C, and particularly at 750°C, lead to partial dissolution of this metastable phase, and its replacement by the stable DOa-type orthorhombic δ phase. The latter, which has been reported in Custom Age 625 Plus [2] and in aged 625 alloy [12-14,18], can form at higher temperatures without the initial presence of γ". Its composition is very close to that of the γ" phase (table IV), and its formation at 750°C does not produce significant softening. However, because of its coarse platelet morphology, it can be expected to entrain a marked loss in ductility.

At low temperatures (550 and 580°C), the alloys B and C both harden after long exposure times, and the presence of titanium does not seem to exert a strong influence on this process. The titanium-containing grade in the hardened condition could be used

for long durations in the temperature range from 500 to 600°C, without significant alteration of its properties. On the contrary, if standard 625 alloy is used in the annealed condition in the same temperature range, the mechanical characteristics could change appreciably over a service life of several years or decades.

4.3 Corrosion resistance

It has been seen that aging produces an increase in the intergranular corrosion rate in the ASTM G 28 A test in alloy B. This sensitization, which is well known for both standard 625 alloy [19,20] and the titanium hardened version [2], is due to the intergranular precipitation of chromium and molybdenum-rich carbides of the type $M_{23}C_6$ and M_6C [12-14,19], which depletes the γ matrix in these elements in the vicinity of the grain boundaries. The nature and composition of the carbides formed during aging were not determined in alloy B, but a statistical study was carried out on a specimen of an industrial heat of standard 625 alloy. Table VI shows the results obtained from the analysis of at least 20 particles of each phase (about 80 particles for $M_{23}C_6$), together with the composition of the γ matrix in the immediate vicinity of the carbides. The MC carbides were formed during annealing at 950°C and the $M_{23}C_6$ and M_6C during a 50 hour aging treatment at 700°C. It can be seen that, for a given type of compound, the composition of the particles varies considerably. All three carbides deplete the matrix in molybdenum, M_6C having the greatest effect. Only M_6C, and especially $M_{23}C_6$, lead to local chromium depletion.

Specimen	Phases		Ni	Cr	Fe	Nb	Mo	Ti	Si
	nominal	wt. %	62.66	20.15	4.42	3.92	8.21	0.19	0.13
	composition	at. %	63.9	23.2	4.74	2.53	5.12	0.24	0.28
carbon	MC		-	1/3	-	73/83	11/15	4/6	0/3
	$M_{23}C_6$	at %	0/11	56/85	-	0/5	11/22	-	0/3
replica	M_6C		20/28	12/30	-	5/11	34/44	-	7/11
thin	γ near MC		65.6	21.3	4.8	1.8	6.5	-	-
	γ near $M_{23}C_6$	wt.%	70.2	13.9	5.1	3.9	6.9	-	-
foil	γ near M_6C		70.5	16.7	5.2	3.0	4.6	-	-

Table VI : Standard* 625 alloy (SUPERIMPHY 625) : composition range of intergranular carbides and examples of γ matrix composition in the vicinity of these carbides (AEM/EDS analysis). (* C= 0,034 %, Al = 0,12 %)

In 625 alloy aged for up to 1000 hours, it has been shown [19] that the sensitivity to intergranular corrosion increases with holding time, as was also found for alloy B exposed for times up to 2048 hours (figure 9). Other nickel base alloys containing 13 to 16 % Mo show similar behaviour [21], whereas in several molybdenum-free grades (alloys 600, 690, 800, X-750, etc.), the sensitivity decreases with time, and disappears after 10 to 20 hours at around 700°C. In these materials, in which the only carbides to form are chromium-rich $M_{23}C_6$ and M_7C_3, the rapid diffusion of chromium quickly restores the composition in the grain boundary regions to a level similar to that of the matrix.In alloy 625, the low diffusion rate of molybdenum in this temperature range, and the fact that $M_{23}C_6$ is gradually replaced by M_6C [13], probably prevents the homogenization of the matrix, and on the contrary, increases the width of the depleted zone on each side of the boundary. It is thus important in this grade to limit the amount of carbon in solution before aging, and therefore to restrict the annealing temperature. For alloy B, it has been seen that the minimum sensitivity occurs for an annealing temperature of 1050°C (figure 8), below which the δ phase apparently exerts a deleterious effect, and above which the secondary MC carbides are taken back into solution. A temperature of this order (1038°C) has been employed by R.B. Frank et al. [1,2] for Custom Age 625 Plus.

However, in alloy B, annealed at 1050°C and aged to produce maximum strengthening (750°C 8h -> 620°C 8h), sensitization occurs nevertheless, if the limiting corrosion rate is taken as 1 mm/yr. It has also been shown (figures 6 and 9) that sensitization in this alloy

always appears at the same hardness, whatever the aging temperature between 620 and 750°C, the critical level being significantly lower than the maximum values attained at these temperatures. A similar phenomenon has been observed by R.B. Frank et al. [2], indicating that there may be a relationship between the quantity of γ" precipitated and the corrosion rate, the effect of this phase adding to that of the intergranular carbides. Table VII shows the calculated composition of the matrix aged at 650 and 750°C, after precipitation of an estimated volume fraction of 10 % γ". It can be seen that only the titanium and niobium contents decrease significantly, while the chromium level has increased slightly. It therefore seems unlikely that the residual matrix is more sensitive than the homogeneous alloy. However, additional studies would be required to confirm that only the intergranular carbide precipitation is responsible for the sensitization in the aged condition.

Condition	Ni	Cr	Fe	Nb	Mo	Ti	Al
Nominal composition	60.18	19.89	4.66	3.70	8.26	1.21	0.15
Aged at 650°C	60.8	21.6	5.20	1.49	8.05	0.76	0.15
Aged at 750°C	59.8	21.9	5.15	1.80	8.49	0.77	0.15

Table VII : Alloy B : calculated composition (wt.%) of the γ matrix after precipitation of 10 % γ" phase at 650 and 750°C.

The most important point is that it is not possible to use the maximum hardening potential in this grade if the corrosion rate must be limited. However, for titanium hardened 625 alloy, a proof stress level of about 900 MPa can be attained for a corrosion rate of 1 mm/yr, using the step aging treatment 732°C 8h -> 620°C 8h preceded by annealing at 1038°C [2].

Conclusions

The addition of about 1 % titanium to alloy 625 increases the amount of Laves phase formed in the interdendritic spaces during solidification. This phase can be dissolved by high temperature soaking above 1150°C, which leads to satisfactory homogenization.

The best compromise between proof stress and impact toughness is obtained by annealing at 1050°C (1h), followed by step aging 750°C 8h -> 620°C 8h (0.2 % P.S. = 1050 MPa, KCV = 10.8 daJ/cm^2). This annealing temperature, which also leads to optimum intergranular corrosion resistance, is sufficiently high to avoid formation of the Ni_3Nb-type δ phase, and low enough to limit grain growth and carbon uptake due to dissolution of the secondary MC carbides. However, in order not to exceed a corrosion rate of 1 mm/yr in the ASTM G 28 A test, the aging temperature and/or time must be limited, restricting the useful proof stress to about 900 MPa.

Long time exposures (~ 2000 hours) at 700°C, and especially 750°C, cause the $Ni_3(Nb,Ti,Mo)$ γ" hardening phase to transform to the stable δ phase, of similar composition, without significant softening. Analogous exposures at about 550°C also produce hardening, with an amplitude and rate of comparable magnitudes in both standard 625 alloy and in the titanium-strengthened grade.

References

1. R.B. FRANK, T.A. DEBOLD, "Custom Age 625 Plus : A New Age - Hardenable Corrosion-Resistant Alloy" (Paper presented at the ASM Materials Conference, Orlando, Florida, 7 October 1986).

2. R.B. FRANK, T.A. DEBOLD, "Heat Treatment of an Age-Hardenable Corrosion-Resistant Alloy - UNS N07716" (Paper presented at Corrosion 90, Las Vegas, Nevada, 23-27 April 1990), 59.

3. E.L. RAYMOND, Trans. A.I.M.E , 239 (1967), 1415.

4. I. KIRMAN, D.H. WARRINGTON, J.I.S.I., 207 (1967), 1264.

5. D.F. PAULONIS, J.M. OBLAK, D.S. DUVALL, Trans. A.S.M., 62 (1969), 611.

6. A. ROYER, (Thèse Docteur es Sciences, Université de Nancy, 1970).

7. W.E. QUIST, R. TAGGART, D.H. POLONIS, Met. Trans., 2 (1971), 825.

8. R. COZAR, (Thèse Docteur-Ingénieur, Université de Nancy, 1973).

9. M.J. CIESLAK, T.J. HEADLEY, T. KOLLIE, A.D. ROMIG, Jr, "A melting and solidification study of alloy 625", Met. Trans, 19A (1988), 2319-2331.

10. M.J. CIESLAK, T.J. HEADLEY, R.B. FRANK, "The Welding Metallurgy of Custom Age 625 Plus Alloy", Welding Research Supplement, 1989, 473-482.

11. G. MARTINEZ, Private Communication With Author, Centre de Recherches de IMPHY S.A., 15 December 1988.

12. F. GARZAROLLI, A. GERSHA, K.P. FRANCKE, Z. Metallkunde, 60 (8) (1969), 643-652.

13. E. SCHNABEL, H.J. SCHULLER, P. SCHWAAB, "The Precipitation and Recrystallisation Behaviour of the Nickel-base Alloy Inconel 625", Practical Metallography, 1971, 521-527.

14. M. SCHIRRA, Metall., 36 (4) (1982), 394-401.

15. F.G. WILSON, F.B. PICKERING, J.I.S.I., 205 (1967), 628.

16. O.H. KRIEGE, C.P. SULLIVAN, Trans. ASM, 61 (1968), 278.

17. O.H. KRIEGE, J.M. BARIS, Trans. ASM, 62 (1969), 195.

18. M. SUNDARARAMAN, P. MUKHOPADHYAY, S. BANERJEE, "Precipitation of the δ - Ni_3 Nb phase in two Nickel Base Superalloys", Met. Trans., 19A (1988), 453-465.

19. J.A. HARRIS, R.C. SCARBERRY, "Effect of Metallurgical Reactions in Inconel Nickel Chromium-Molybdenum Alloy 625 on Corrosion Resistance in Nitric Acid", Journal of Metals, 1971, 45-49.

20. M.H. BROWN, "The Relationship of Heat Treatment to the Corrosion Resistance of Stainless Alloys", Corrosion, 25 (10) (1969), 438-443.

21. U.L. HEUBNER, E. ALTPETER, M.B. ROCKEL, E. WALLIS, "Electrochemical Behavior and its Relation to Composition and Sensitization of NiCrMo Alloys in ASTM G-28 Solution, Corrosion, 45 (3) (1989), 249-259.